FROST
Far infraRed Observation Spectography Telescopes

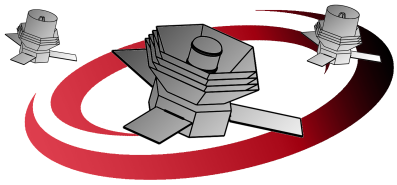

FROST

Far-infraRed Observation Spectroscopy Telescopes

C. Bolart, M. Brehaus, L. Estanqueiro, C. Fröhlich, M. Guyot, B. Hegyesi, E.W. Knutsen, V. Lauksio, G. de Marco, S.H. Owe, O. Price, O. Pinzon-Rodriguez, S. Wagner, I. Zankov, M. Ziebart

Science tutor: Michael Mach *Engineering tutor:* Luzius Kronig

July 26, 2017

Abstract

In this report we propose a mission to observe the inner protoplanetary disks of T Tauri and Herbig Ae/Be stars in the far infrared wavelengths from 40 to 200 μm at distances up to 140 pc at high angular resolution. FROST (Far-infraRed Observation Spectroscopy Telescopes) will be a three part formation flying interferometer, which will orbit the second Lagrangian point, and provide spectroscopic observations. The telescopes will be equipped with FIR Interferometers coupled with Fourier Transform Spectroscopy so as to retrieve the spectrum. Dichroic mirrors will split the light beams into different ranges in order to analyse them for chemical composition. FROST will be able to observe at least 78 disks in the Milky Way with a spatial resolution of up to 0.7 AU and a spectral frequency resolution of $R = 1600$ (0.1 μm bins) in order to detect shifts in silicate features in the disks emission spectra. This mission will provide information about the size distribution, structure and chemical composition of grains along the disk in order to trace its evolution. This paper explores the difficulties involved in such a concept and demonstrates it's feasibility by making science-engineering trade-offs with regards to instrumentation and procedure

1 Introduction

Protoplanetary disks were discovered by C. Robert O'Dell [1] in 1994 with the Hubble Space Telescope (HST) observations. Since then, they have been observed by several ground based and space telescopes, but never with the resolution FROST offers.

These dense circumstellar disks have been found to be a mixture of dust and gas orbiting young stars, and evidence suggests that they are the places where new planets are born[2].

Being able to understand the processes in protoplanetary disks will give us valuable information in order to understand the mechanisms behind planet formation, and the origin of Earth itself.

2 Scientific Background

Protoplanetary disks are found in star forming nebulas. As the material from the diffuse ISM self gravitates, it becomes denser and starts to fragment, collapse and rotate[3]. A protoplanetary disk will then form around the central young stellar object. The flat

structure of the disk is due to conservation of angular momentum.

Understanding the dust mass, the grain size distribution, grain structure (crystallinity, "fluffiness") and the chemical composition - all as a function of position in the disk - remains the main challenge in the fields of disk evolution and planet formation[2]. Answering these questions requires both IR and submillimeter observations, since observations at these wavelengths are sensitive to fundamental disk properties [4].

3 Scientific Objectives

3.1 SO-01: Grain Size Distribution.

The grain size distribution across the disk will give us information on where and how planets are formed in the disk [3]. This distribution will be determined from measurements of the shape of the Spectral Energy Distribution and comparison with models, which has been studied before by P. Woitke in 2016 (See Figure 1).

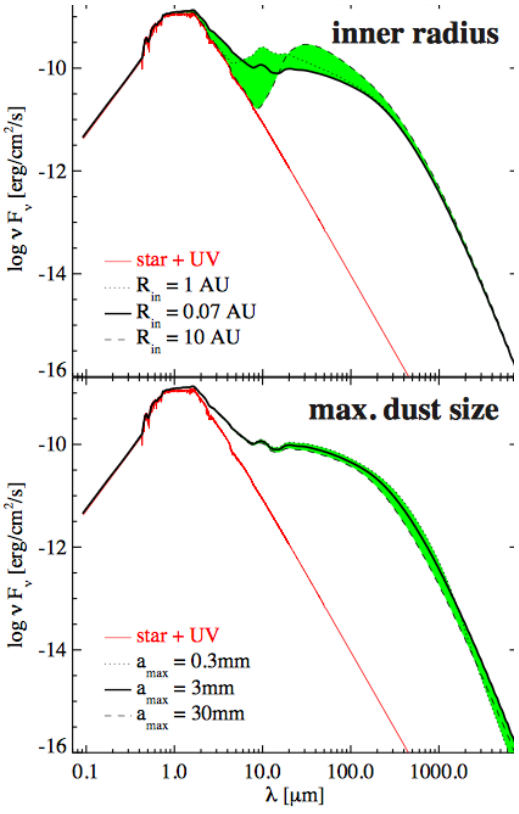

Figure 1: Comparison of dust and disk parameters on models of SED at distance 140 pc

3.2 SO-02: Temperature Gradient.

The temperature profile across the disk controls the chemical and physical processes affecting dust[3]. These gradients determine the structure and composition of grains as they enter the protoplanetary disk and move closer to the forming star. We will determine the temperature gradient measuring the shift in wavelengths of several spectral features.

3.3 SO-03: Chemical Composition.

The chemical composition of the dust grains will be interpreted from the various features which will appear on the continuum. We expect silicate peaks from 40μm, ice features between 40-120 μm, and atomic emission lines like [CII] at 158 μm and [OI] at 63 μm & 145 μm [5].

3.4 SO-04: Frost Line

Models show a change in dust distribution somewhere between 2 and 3 AU. This is the area where important volatiles such as water vapour reach their condensation temperatures. It is theorised that this plays a major role in grain growth, as the ice makes the dust "sticky". The rapid grain growth makes this region suitable for the formation of planetoids.[6] The only observed frost line was seen at 42 AU, when the star V883 Ori had a violent outburst. An abrupt change in optical depth was measured, in the region where the temperature is closing in on the condensation point of water. We wish to observe frost lines in their natural position, and observe grain growth as well as search for gaps in the disk.

3.5 Observation Plan

FROST will observe inner protoplanetary disks in the Milky Way within 140 pc. However, the distribution of the objects within this distance is not uniform along the galactic plane. This means that there are regions in the spacecrafts' of sight that are more dense than others. For this reason, two approaches are necessary. FROST is going to: (1) do short-term observation of many targets in high-density regions, and (2) trace objects in low-density regions for longer periods of time (e.g. TW Hya can be observed for approximately 2 months) in order to detect changes in its structure.

3.5.1 Secondary Science

Since the number of stars with protoplanetary disks are not distributed uniformly around FROST's field of view, some downtime is inevitable. During this period the telescope can observe Active Galactic Nuclei (AGNs). This will provide informations about the dust size distribution of the dusty torus, which is believed to be part of most of the AGNs. Knowledge about the dust size distribution can prove theories about the composition of the torus, and will be very important to prove or disprove the unification model for AGNs [7].

3.6 Scientific Requirements

3.7 SR-01: Number of Targets.

We have catalogued 78 objects we want to observe, 75% T Tauri (<2 M_{sun}) and 25% Herbig Ae/Be (2-8 M_{sun}) stars. Previous observations mean their structure and inclination is well known. This catalogue will provide us the amount of information needed for detailed research of star and planet formation processes.

3.8 SR-02: Upper Distance Limit.

The nearest star forming clouds are found within 140 pc from us. In this regions many interesting protoplanetary disks can be observed. For this reason, this distance has been set as FROST observation limit.

3.9 SR-03: Minimum Flux.

The estimated targets flux range from 1×10^{-12} to $1\times10^{-9} ergcm^{-2}s^{-1}$, depending on the star. We require the instrument to absorb enough photons to resolve a flux in the middle of this range; $1\times10^{-11} ergcm^{-2}s^{-1}$.

3.10 SR-04: Spatial Resolution.

The frost line of protoplanetary disks have been theorized to start at a distance from the star of 2-3 AU[6]. In order to resolve how the properties of the disk change from 1 to 5 AU, a spatial resolution of less than 1 AU is needed. This must be possible at a distance of 140 parsec. The spatial resolution of FROST is 0.7 AU.

3.11 SR-05: Disk Size.

Silicate features may be found from 10 μm, and further out throughout the disk. At the frost line, the intensity from silicates is thought to drop, due to covering from ice particles. It is in the region around the frost line where rocky planets like our own is thought to form.

3.12 SR-06: Reference Wavelength.

Forsterite features show up at 69 μm [8], in a large part of the catalogued stars. The spectral features contain information about chemical composition, grain size and temperature, and can be used to constrain the physical location of forsterite in the disk.

3.13 SR-07: Wavelength Interval.

Dust emissions peak at 100 μm, and as mentioned a reference wavelength of 69 μm was chosen. The JWST will observe protoplanetary disks from 0,6 to 28 μm [9].

3.14 SR-08: Signal to Noise Ratio.

The observed continuum flux is of the order 10^{-12} erg cm^{-2} s^{-1}, while the feature emission equal to 10^{-10} erg cm^{-2} s^{-1}. In order to resolve the 69 μm features from the continuum, the signal to noise ratio has to be equal to 100.

3.15 SR-9: Spectral Resolution.

Temperature measurements require the detection of shifts in the spectral peaks. The smallest observable shift in the silicate features are 0.1 μm [5]. These shift indicates a temperature change of approximately 50 K.

4 Payload

4.1 Implementation

To meet the science requirements of high spatial and spectral resolution (SR-04, SR-09), a large baseline interferometer is required, with FTS. The interferometer must be space born since the atmosphere of Earth is opaque to the waveband from the science requirement (SR-07). The interferometer will consist of three free-flying spacecraft, due to requirement on

the length of the baselines neccesary for the high spatial resolution (SR-04). These baselines are too large to make use of a boom. The interferometer in itself is a simple three-spacecraft system consisting of two Light Collecting Spacecraft's (L CS) and one Beam Combination Spacecraft (BCS) where the light from the two LCS will be combined through FTS.

rived by (PL-04). This takes into consideration two mirrors and the requirement resolution given by (SR-09). For 15 baselines and the estimated time for recalibration as well as repositioning, the overall observation time per objects is 32.5 hours.

4.2 Interferometer Design

The basic principle of the payload is to do far infrared spectroscopy using interferometry with FTS. The implemented solution utilises three free-flying spacecraft's, with two LCSs and one BCS combining the beams and performing the FTS. The principle of interferometry is to utilize the information of the interfering light. If two waves which are in phase are combined, the signal will get larger, and if two waves out of phase are combined, the signal will amplifies. The FTS exploits this principle to determine the intensity of wavelengths by applying a time variable delay to one of the two beams being combined. The longer the physical path of this delay, the better a resolution can be achieved. The outcome is an interferogram, which after a Fourier Transform will become a spectrum.

4.2.1 Light Collecting Spacecraft Design

The role of the LCS is to gather light from a target and direct this light towards the BCS. The physical distance between the two LCS is the baseline of the interferometer. The distance between each LCS to the BCS needs to be completely equal, since the light must travel an equal distance before recombination. Inside the LCS is a primary and a secondary mirror focusing the light to a focal point. The primary mirror is of diameter 2 m (PL-04). Around the focal point a field stop is placed to avoid stray light. Before the focal point another mirror is placed to reflect light to a near infrared detector which works as a fine guidance sensor. After the focal point a collimator is placed collimating the light to a diameter of 3 cm (PL-11). Inside LCS there will also be tip-tilt mirrors (PL-05) for directioning of the light. On Figure 2 a schematic of the LCS is illustrated.

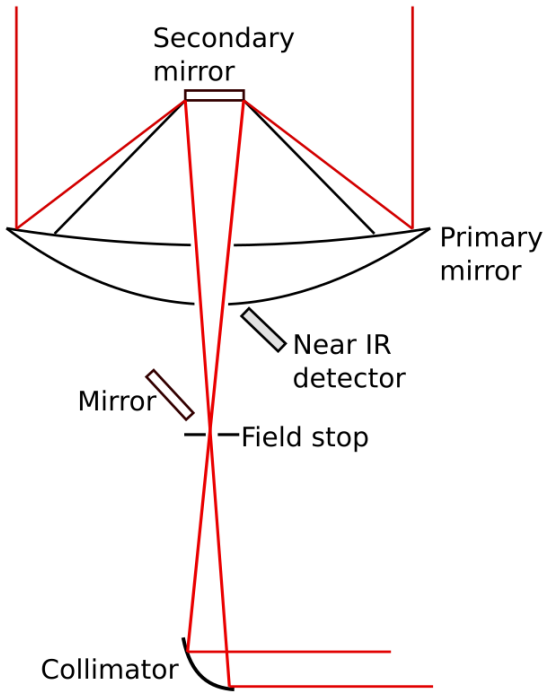

Figure 2: Schematic of LCS

4.2.2 Beam Combining Spacecraft

In the BCS the FTS is performed by combining the light arriving from the two LCS's. When light enters the BCM it will arrive first at the combiner primary and then the combiner secondary mirror. From here the OPD resulting from spacecraft positioning errors, will be corrected by directing the light through a constantly correcting delay line system. This delay line system shall be similar to the one developed for the DARWIN mission. This system has sub nm precision and must be cooled to 40 K. The mirror in this delay line shall be a corner cube retro reflector [10]. Next the beam will arrive at a tip tilt mirror, which directs the beam towards the FTS system. Taking advantage of dichroic mirror technology, the wavelengths below 40μm will be directed to an interferometer used for position measurement between the spacecraft's (PL-09). Next the FTS will be performed with sets of dichroic mirrors splitting the light in four different wavebands to four detectors (PL-06). Using a similar delay line system as for the OPD correction between the spacecraft's [10], the variable time delay is performed on the light coming from one LCS while the other is constant. This delay line system needs to be able to delay the light with a distance of 20 cm to get the required spectral resolution (PL-07). To minimize the integration time the light will be divided into four

bands being observed simultaneously - yielding four detectors. As a result an interferogram is obtained. Every interferogram must be corrected to the calibration. A Fourier Transform of the interferogram provides the measured spectrum with $0.1\mu m$ spectral resolution[11]. Every time the baseline is changed, the detectors must be calibrated using a cold source (4K) and a blackbody. On Figure 3 a schematic of half of the FTS system is illustrated.

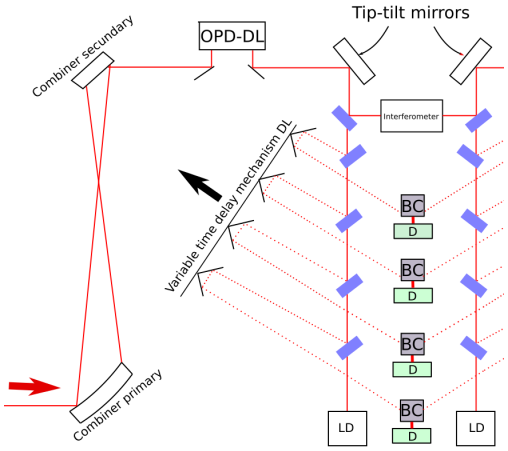

Figure 3: Half of the FTS system. The system is symmetrical, but light coming from the right will not be delayed.

The key mission drivers of the payload is to perform free flying interferometry in space, to the perfection of the required pointing accuracy, and baseline stability to perform a successful beam combination procedure. Also the delay line system must perform perfectly.

5 Mission Analysis

5.1 Launch and Orbit

A large-amplitude Lissajous orbit around the L2 point is chosen, with a semi-axis of 8×10^5 km, allowing for solar eclipses to be completely avoided. This ensures constant solar power and lower solar radiation. This orbit requires lower delta-v (100 m/s per spacecraft) for orbit insertion and maintenance. This orbit was chosen because it offers low station keeping costs, low perturbations (crucial for formation flying), a constant distance to earth (i.e. constant max. data rate) and is in a low radiation environment.

The proposed launch system is the Ariane 6-4 rocket, with a direct insertion orbit into L2. The three spacecraft are stacked onto each other in the launcher with a special manufactured structure holding them together. A few hours after the launch, the spacecraft are separated from the launcher and then two orbit correction burns are performed with the first spacecraft on the stack. Only after these correction burns do the spacecraft separate and fly in formation to the targeted orbit in L2.

5.2 Formation Flight Control Subsystem

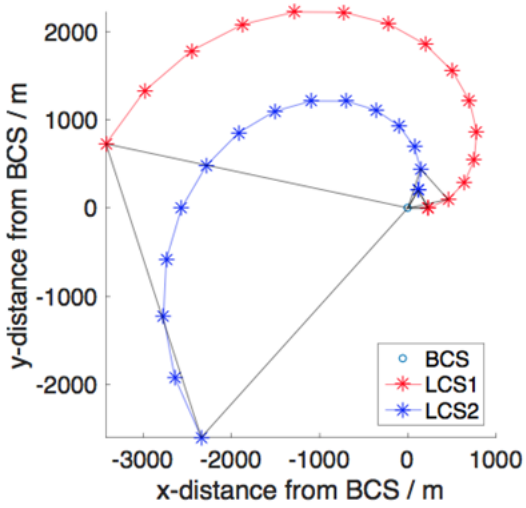

Figure 4: Changing of the size and orientation of the baseline for one target observation

The interferometer needs measurements with different distances and orientations between the light collecting satellites. This is achieved by controlling the satellites in an equilateral triangle. This formation is held precisely during scientific measurements. After the measurement the satellites are repositioned in order to change the baseline distance whilst keeping the orientation perpendicular to the target. This is achieved by maintaining the beam combining satellite on its orbit and by repositioning the two light collecting satellites. During the observation the satellites are capable of maintaining a relative distance stability of less than 10 μm. They can measure the distances with an absolute error of less than 10mm and a relative error in the nanometer range. This is achieved by the use of cold gas thrusters and a two stage metrology system. The first stage uses a radio based system developed by CNES and used on PRISMA, which is capable of determining the satellites positioning to centimeter accurac, ensuring correct initial positioning. The second stage uses the

ULLIS precision system with an absolute position accuracy of less than 100 μm in combination with the Fine Relative Lateral Sensor system. It provides a relative measurement accuracy of a few nanometers.

6 Spacecraft

6.1 ADCS Subsystem

The spacecrafts have to face in a precise direction during observation, so it has to be three-axis stabilized design. Six Sun sensors, two star trackers and one fybergyro are necessary to compute the angular position of each spacecraft. On every LCS there is also a Fine Guidance Sensor to achieve the desired accuracy, while in the BCS this precision is achieved by two high precision star trackers. Four 8 Nms reaction wheels and twelve cold gas thrusters are used to maintain the attitude and to counteract the solar radiation pressure torque. The absolute angular accuracy is 0.43".

6.2 Propulsion Subsystem

Maneuver	LCS Δv ($\mathrm{m\,s^{-1}}$)	BCS Δv ($\mathrm{m\,s^{-1}}$)
Coarse-propulsion system		
Orbit insertion and launcher dispersion[12, 13]	25	100
Reconfiguration and retargeting	325	-
Station keeping incl. wheel unloading	12	12
Disposal[14]	25	25
Sum	387	137
micro-propulsion system		
Formation Flight Precision Control	5.5	5.5
Solar pressure compensation	0.5	0.5
Sum micro-propulsion system	6	6

Table 1: Coarse-propulsion Δv budget

The mission requires fast reconfiguration between the observations whilst achieving high accuracy during observations. A two-staged propulsion system is hence proposed. The coarse-propulsion system has higher thrust and impulse to achieve fast movements. The thrusters are of mono-propellant type, and hydrazine is used to generate the thrust. Hydrazine has higher specific impulse and therefore, less overall propellant mass is needed. The calculated Δv budget is shown in Table 6.2, what results in 335 kg hydrazine for the LCS and 250 kg for the BCS, respectively. For the micro-propulsion system cold gas is used. mN-thrusters with a high resolution for fine positioning are used, providing the thrust ranging from 1 µN to 1000 µN. For the micro-propulsion system 20 kg of Nitrogen had been calculated.

6.3 Thermal Control Subsystem

The high sensitivity of the optics requires a suitable thermal control subsystem. The subsystem will employ both a passive and an active cooling method, owing to the desired detector temperature being at or beneath 50 mK. Passive cooling is implemented by using multilayer insulation (MLI). The structure containing payload instruments is shielded on all sides, significantly decreasing the radiation flux reaching the payload structures, originating from the "warm zone" of the spacecraft. The warm zone consists of a section of the spacecraft containing the less heat sensitive equipment that is warmed from a fraction of the incoming solar radiation, the propulsion subsystem, and the heat from nearby electronics. The side separating this zone from the outside will be an type MLI shield comprised of aluminium and doped in silicon (keeping the emissivity at around 0.05) to reflect as much incoming radiation as possible. On the other side of the warm zone comes the second part of the passive half of the TCS – a V-groove MLI array built to minimise warm zone radiation leaking into the instrument bank. This still is not enough to drop the operation temperature lower than the 45 K minimum that passive cooling can offer, so a multi-stage active cooler is needed. If the stages consist of repeated compression and adiabatic demagnetisation, then the system can be cooled down to 50 mK without a short-lived cryogenic coolant ever being necessary. The active cooling system should be quite similar to the one proposed for the Athena mission.

6.4 Power Subsystem

The spacecrafts use as secondary energy source triple-junction GaAs solar cells with a conversion efficiency of 20% at beginning-of-life. [15] Sony 18650HC Li-ion batteries in a 46p9s configuration provide power during orbit injection phase and in case of peak power needs. They have 2.6 kWh capacity, depth-of-discharge of 40 % and 5 hours of autonomy. The buses are 28 V fully regulated.

6.5 On-Board Computer

The ADCS system requires a powerful On-Board Computer. ICDE-NG (Integrated Control and Data Equipment-Next Generation) was chosen as a flight-proven, 32-bit based, fully redundant On-Board Computer [16].

6.6 Telecom Subsystem

Each spacecraft has two low gain antennas (LGA) and the beam combining spacecraft (BCS) one medium gain antenna (MGA) with gimbal for high data rate transmission of science data to ground stations. The target data rate for the science data downlink is 50 Mbps. To do this, two parabolic antenna have been selected. They are on the BCS spacecraft and have a diameter of 20 cm. The gain is 22.4 dB.

6.7 Mass

Spacecraft masses are presented in table 2 on subsystem level is divided in subsystems.

Subsystem	Mass w/ cont. [kg]	
	BCS	**LCS**
Structural	291	386
Electrical	168	168
Telecom	20	0.6
AOCS	328	328
Propellant	364	503
Satellite bus	99	99
Thermal control	441	9
Payload	259	534
Whole S/C	1670	1752
Fairing structures	313	
Adapter	125	
Constellation total	6006	

Table 2: Mass budgets for both spacecraft types. All values include proper part level contingencies and 20% contingency for all subsystems.

6.8 Dimensions

The light collecting spacecraft has a height (Z-axis) of 4.35 m and a diameter (X- and Z- axes) of 3.034 m. The beam collecting spacecraft has the same height as LCS, but a diameter of 2.43 meters.

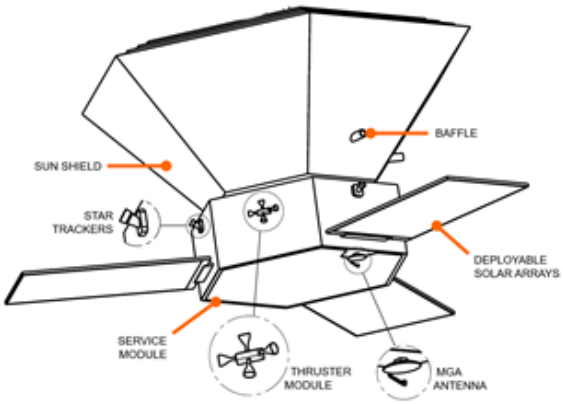

Figure 5: LCS Spacecraft

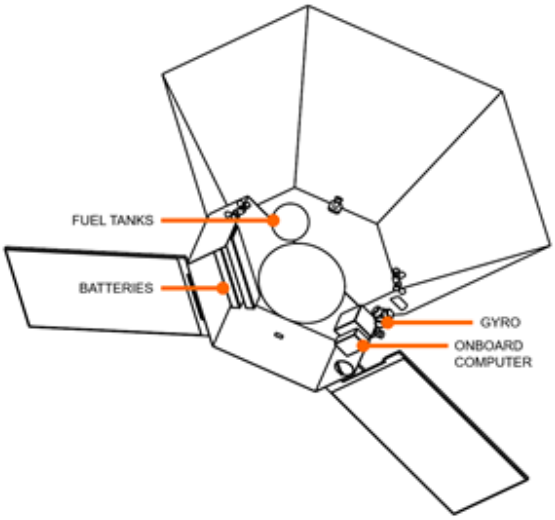

Figure 6: Cross section of the S/C

7 Operations and Ground Segment

The selected ground stations are Cerebro (Madrid) and New Norcia (Australia). They has been used to support Mars Express, Rosetta, etc. They have both 35m deep-space antenna with transmission and reception in both S and X-band. They are in different hemispheres and can be used to provide a link to Earth in winter as well as in summer.

8 Cost and Risk Assessment

Spacecraft costs and risks are assessed in this section. Herschel is used as a comparative source and PROBA-3's projected technology demonstration is

used as a means to determine the TRL development costs as well as mission risks.

8.1 Cost Assessment

In order to achieve a good cost estimate, the mission's service module is compared to other similar projects like the Herschel according to similarities and differences, in order to estimate costs. Separately, the payload module's cost is calculated on the same comparative basis. Assuming that ESA Project Operations represents 20% of Spacecraft Payload costs, and a 15% contingency on ESA Project Office, SpaceCraft, and Operations costs. The final cost figure is shown on Table 3. PROBA-3 mission is already developing critical technology, which will drive down the costs for the FROST project.

Description	**Million Euros**
SpaceCraft 1 SVM	300
SpaceCrafts 2 and 3 Telescope	510
2 Telescopes, PLM, FGS	250
Total Industrial Cost	**1060**
Payload MI, FGS, metrology	350
Cooling 50mK	100
Total Payload	**450**
Project Operations ESA	212
Spacecraft	1060
Operations	170
Launcher	175
Contingency 15%	216
Total ESA CaC	**1833**
Payload (Member States)	**450**
Total Cost	**2283**

Table 3: Cost Estimate Table

8.2 Risk Assessment

First, the TRL of the technologies are analysed as well as their relation to key mission drivers. ESA's ongoing PROBA-3 mission is a formation flying technology demonstrator. This means that the biggest risks - associated with precision formation flying- will diminish as their associated technologies rise in TRL rankings during PROBA-3's timeline. These technologies mature into high TRL levels one year into project phase A.

Technology	**TRL**
OPD Correction system	TRL5
Detector	TRL5
Free flying Interferometer	TRL5
Telescope	TRL8
Propulsion system	TRL9
AOCS subsystem (formation flight)	TRL4
Telecom subsystem	TRL9
Electric power subsystem	TRL9
Metrology	TRL5

Table 4: Technology Readiness Level (TRL)

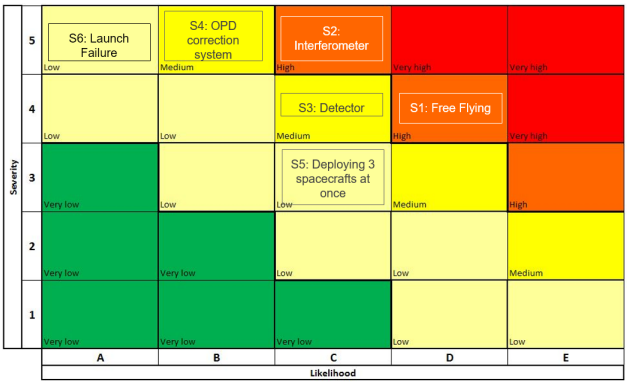

Figure 7: Risk assessment figure.

9 Outreach Plan

The outreach is sub-divided into two distinct, complementary approaches. They are social media for influencing public opinion, and crowdfunding for additional funding.

9.1 Social Media

The plan involves creating a FROST Telescope twitter account as well as a FROSTelescope Facebook page to keep the population updated on everything related to the project. Also, a special SnapChat filter will be made available worldwide to celebrate the occasion.

9.2 Crowdfunding

The plan involves creating a crowdfunding campaign with donation goals set for rewarding generous donations. The reward proposals for involve 'naming a baby planet' as well as setting up a plate with donator's names on them to be sent into space. All the money received from this outreach approach is an extra incentive to the program which will alleviate ESA

costs as well as promote a closer link between the public, scientists and the mission. With enough public interest and crowdfunding, it is possible to create further outreach initiatives such as travelling exhibitions targeting children and adults.

10 Conclusion

The FROST mission will provide information of properties such as size, distribution and composition of dust grains in protoplanetary disks within 140 pc in order to better understand the mechanisms behind planet formation. This represents one of the main remaining challenges in astrophysics and FROST will be able to fill this gap in our knowledge.

The proposed technology is necessary for further progress in high spatial and spectral resolution in the far IR regime. The FROST concept will not perform imaging interferometry, which relaxes various design parameters. Performing a formation flying three-spacecraft constellation to accomplish a Fourier Transformation Spectroscopy to scan planetary disks is as challenging as it is rewarding. This will open the door for future high spatial resolution mission.

References

[1] C. R. O'Dell. "The Orion Nebula: structure, dynamics, and population". In: *Astrophysics and Space Science* 216 (1994), pp. 267–280.

[2] Sebastian Wolf, Amaya Moro-Martín, and Gennaro D'Angelo. "Signatures of planets in protoplanetary and debris disks". In: *Planetary and Space Science* 55.5 (2007), pp. 569–581.

[3] C John, LEISAWITZ David, et al. "The SPIRIT and SPECS Far-Infrared/Submillimeter Interferometry Missions". In: *title The Institute of Space and Astronautical Science repot. SP* 14 (2000), p. 219.

[4] S.A. Metchev J.H. Kastner B. Stelzer. "The Structure and Evolution of Protoplanetary Disks: an infrared and submillimeter view". In: *Young Stars and Planets Near the Sun* 314 (2015), p. 7.

[5] B Sturm et al. "First results of the Herschel key program "Dust, Ice and Gas In Time"(DIGIT): Dust and gas spectroscopy of HD 100546". In: *Astronomy & Astrophysics* 518 (2010), p. L129.

[6] Lucas A Cieza et al. "Imaging the water snow-line during a protostellar outburst". In: *Nature* 535.7611 (2016), pp. 258–261.

[7] S. Bianchi, R. Maiolino, and G. Risaliti. "AGN Obscuration and the Unified Model". In: *Advances in Astronomy* 2012, 782030 (2012), p. 782030. DOI: 10.1155/2012/782030. arXiv: 1201.2119.

[8] KM Maaskant et al. "Location and sizes of forsterite grains in protoplanetary disks-Interpretation from the Herschel DIGIT programme". In: *Astronomy & Astrophysics* 574 (2015), A140.

[9] Jonathan P Gardner et al. "The james webb space telescope". In: *Space Science Reviews* 123.4 (2006), pp. 485–606.

[10] TC Van den Dool et al. "The DARWIN breadboard optical delay line verification programme". In: *Proc. SPIE*. Vol. 6268. 2006, 62682O.

[11] VA Iafolla et al. "FISICA (Far Infrared Space Interferometer Critical Assessment) metrological problems and system requirements for interferometric observations from space". In: *Metrology for Aerospace (MetroAeroSpace), 2014 IEEE*. IEEE. 2014, pp. 161–166.

[12] C. Ruilier, M. Sghedoni, and R. Krawczyk. *DARWIN System Assessment Study Summary Report (DW-SAS-ASP-TN-457)*. Tech. rep. Alcatel Alenia Space, 2007.

[13] Martin Hechler and Arturo Yanez. *Herschel/Planck Consolidated Report on Mission Analysis (PT-MA-RP-0010-OPS-GMA)*. Tech. rep. European Space Agency, 2006.

[14] Camilla Colombo et al. "End-of-life disposal concepts for Libration Point Orbit and Highly Elliptical Orbit missions". In: *Acta Astronautica* 110 (2015). Dynamics and Control of Space Systems, pp. 298 –312. ISSN: 0094-5765. DOI: http://dx.doi.org/10.1016/j.actaastro.2014.11.002.

[15] Peter Fortescue, Graham Swinerd, and John Stark. *Spacecraft systems engineering*. John Wiley & Sons, 2011.

[16] *Datasheet of ICDE-NG On-Board Computer*. Airbus Defense and Space. URL: https://spaceequipment.airbusdefenceandspace.com/wp-content/uploads/2015/04/icde-ng-datasheet.pdf.